Carbohydrate Polymers 92 (2013) 1470–1476

Contents lists available at SciVerse ScienceDirect

Carbohydrate Polymers

journal homepage: www.elsevier.com/locate/carbpol

Chitosan–hyaluronan/nano chondroitin sulfate ternary composite sponges for medical use

B.S. Anisha, Deepthi Sankar, Annapoorna Mohandas, K.P. Chennazhi, Shantikumar V. Nair, R. Jayakumar*

Amrita Centre for Nanosciences and Molecular Medicine, Amrita Institute of Medical Sciences and Research Centre, Amrita Vishwa Vidyapeetham University, Kochi-682 041, India

ARTICLE INFO

Article history:
Received 21 July 2012
Received in revised form 22 October 2012
Accepted 22 October 2012
Available online 9 November 2012

Keywords:
Chitosan
Hyaluronan
Chondroitin sulfate nanoparticles
Nanocomposite sponge
Wound dressing

ABSTRACT

In this work chitosan–hyaluronan composite sponge incorporated with chondroitin sulfate nanoparticle (nCS) was developed. The fabrication of hydrogel was based on simple ionic cross-linking using EDC, followed by lyophilization to obtain the composite sponge. nCS suspension was characterized using DLS and SEM and showed a size range of 100–150 nm. The composite sponges were characterized using SEM, FT-IR and TG-DTA. Porosity, swelling, biodegradation, blood clotting and platelet activation of the prepared sponges were also evaluated. Nanocomposites showed a porosity of 67% and showed enhanced swelling and blood clotting ability. Cytocompatibility and cell adhesion studies of the sponges were done using human dermal fibroblast (HDF) cells and the nanocomposite sponges showed more than 90% viability. Nanocomposite sponges also showed enhanced proliferation of HDF cells within two days of study. These results indicated that this nanocomposite sponges would be a potential candidate for wound dressing.

1. Introduction

Characteristics of an ideal sponge to serve as scaffolds for biomedical applications, it should be non toxic, biodegradable, non allergic, and should allow proper nutrient and gas exchange (Jayakumar, Prabaharan, Sudheesh Kumar, Nair, & Tamura, 2011). Nowadays natural biomaterials are profoundly used over synthetic materials in biomedical applications such as tissue engineering, wound care, drug delivery etc. because of its biocompatibility, biodegradability, and bioactivity which makes it readily integrate with the host tissue (Nair & Laurencin, 2007). Specifically in wound care, natural biomaterials like collagen (Wang et al., 2008), alginate (Shalumon et al., 2011), chitosan (Mi et al., 2001), hyaluronan (Kondo & Kuroyanagi, 2012), etc. are being widely used. Advantages of these materials are low toxicity and non immunogenicity (Anilkumar et al., 2011). Wound care products can be in the form of scaffolds (Madhumathi et al., 2010), membranes (Wang, Khor, Wee, & Lim, 2002), sponges (Kondo & Kuroyanagi, 2012; Mi et al., 2001), hydrogels (Boucard et al., 2007), etc. Sponges are soft and flexible scaffolds with interconnected porous structure having good fluid absorption capability and cell interaction making it a suitable material for wound dressing (Jayakumar et al., 2011).

Chitosan is a cationic biopolymer composed of glucosamine and N-acetyl-glucosamine. It is obtained by the partial deacetylation of chitin (Jayakumar, Menon, Manzoor, Nair, & Tamura, 2010; Muzzarelli, 2009). Chitosan is biocompatible and biodegradable with haemostatic properties, which makes it a potential candidate in the wound management area (Anilkumar et al., 2011; Jayakumar et al., 2011). Polysaccharide backbone of chitosan also shows structural similarity with glycosaminoglycans (GAGs) (Peter et al., 2010). Hyaluronan (HYA) and chondroitin sulfate are GAGs which are the major constituents of the skin extracellular matrix (ECM) (Anilkumar et al., 2011). HYA is a polyanion composed of repeating disaccharide units of N-acetyl-D-glucosamine and glucuronic acid (Kogan, Soltes, Stern, & Gemeiner, 2007). HYA has a high capacity to retain water that provides a moist environment and protects the wounded tissue surface from dryness and promotes wound healing (Kogan et al., 2007). Moreover HYA is shown to have a positive effect in scarless wound healing. A recent study has shown that exogenous HYA when incorporated into fibrin pad improved wound healing with minimum scar in rabbit ear model (Anilkumar et al., 2011). N-acetyl-D-glucosamine, one of the degradation products of both chitosan and HYA promotes fibroblast proliferation and ordered collagen deposition thus facilitating faster wound healing and reduced scar formation (Jayakumar et al., 2011). Chitosan being cationic in nature can form polyelectrolyte complex with HYA which is a polyanion and scientists have hypothesized that the incorporation of HYA to chitosan could enhance the structural and biological properties of the scaffold. Moreover scaffolds

* Corresponding author. Tel.: +91 484 2801234; fax: +91 484 2802020.
E-mail addresses: rjayakumar@aims.amrita.edu, jayakumar77@yahoo.com (R. Jayakumar).

0144-8617/$ – see front matter © 2012 Elsevier Ltd. All rights reserved.
http://dx.doi.org/10.1016/j.carbpol.2012.10.058

containing both chitosan and HYA were found to enhance cell adhesion (Muzzarelli, Greco, Busilacchi, Sollazzo, & Gigante, 2012).

Chondroitin sulfate is an anionic polyelectrolyte composed of alternating units of glucuronic acid and N-acetyl-galactosamine and is sulfated at either 4- or 6-position of N-acetyl-galactosamine residue (Kirker, Luo, Nielson, Shelby, & Prestwich, 2002). It accelerates wound healing by enhancing the influx of fibroblast into the wound (Gilbert et al., 2004). But the exact role of GAGs in wound healing is yet to be unraveled (Kirker et al., 2002). Nanoparticles possess high surface area to volume ratio which stimulates the interaction between biomaterials and cells (Peter et al., 2010). Thus the presence of chondroitin sulfate in the nano form would enhance the fibroblast migration, further supporting fibroblast attachment and proliferation.

In this study, by assimilating the properties of its parent polymers we attempt to develop a chitosan–HYA/nCS ternary nanocomposite sponge for medical applications.

2. Experimental

2.1. Materials

Chitosan (MW 100–150 kDa, degree of deacetylation-85%) was purchased from Koyo chemical, Co Ltd (Japan). HYA was purchased from Qingdao Haitao Biochemical Co Ltd (China). Chondroitin sulfate was received from India Sea food, Kochi. Glutaraldehyde and hen lysozyme were obtained from Fluka, N,N-(3-dimethylaminopropyl)-N-ethyl carbodiimide (EDC) and Acetic acid from Sigma–Aldrich. Human dermal fibroblast (HDF) and its media were purchased from Promo Cell, India.

2.2. Preparation of chitosan–HYA/nCS composite sponge

2.2.1. Preparation of chitosan–HYA blend

Chitosan 2% (w/v) was dissolved in 1% acetic acid; this solution was neutralized with 1N NaOH to obtain chitosan hydrogel. HYA 1% (w/v) was dissolved in double distilled water. These two were mixed in 2:1 ratio to obtain a homogenous chitosan–HYA blend.

2.2.2. Preparation of chondroitin sulfate nanoparticle (nCS)

nCS suspension was prepared by polyelectrolyte ionic cross-linking method as reported by Yeh, Cheng, Hu, Huang, and Young (2011) with modifications. Initially the pH of 0.1% of chondroitin sulfate aqueous solution was reduced to 2. Under continuous stirring 0.05% chitosan in acetic acid solution was added until turbidity was observed.

2.2.3. Preparation of composite sponge

To the chitosan–HYA blend, nCS suspension (10% of chitosan–HYA blend) was added and stirred for 4 h to obtain a homogenous mixture. The resulting slurry was then poured into a mould, freezed and lyophilized for 24 h. The composite sponge was cross-linked with N,N-(3-dimethylaminopropyl)-N-ethyl carbodiimide (EDC) (Sigma–Aldrich) as reported (Park et al., 2003; Collins & Birkinshaw, 2011).

2.3. Characterization

Size of nCS was analyzed using DLS (DLS-ZP/Particle Sizer Nicomp^{TM} 380 ZLS particle sizing system). Measurements were carried out under a monochromatic, coherent laser source emitting at 632.8 nm, and the scattered intensity was measured. Size and morphology of nCS was analyzed using SEM (JEOL Ltd., JEOLJSM-6490LA) for which nCS suspension was diluted in distilled water and mounted on carbon-taped aluminum stubs, which was then gold sputtered (JEOL, JFC-1600) before imaging. The structural morphology of the composite sponges was analyzed using SEM. The sponges were sliced into thin sections to expose its internal architecture. Samples were then mounted on carbon-taped aluminum stubs and gold sputtered before imaging by SEM. To analyze the various functional groups present in the composite sponges, FT-IR measurements were performed using a FT-IR spectrometer (Perkin-Elmer RX1). The samples were finely ground and mixed with potassium bromide and pelletized. The pellets were scanned in the range of 400–4000 cm^{-1}. Thermal stability of the composite sponges were analyzed using TG/DTA instrument (EXSTAR-SII TG-DTA 6200). 3 mg samples were subjected to heating from 25 to 500 °C at a rate of 10 °C/min.

2.4. Porosity

Porosity of the sponges was determined using liquid displacement method. Dimensions of the sponges were measured using a vernier caliper and volume (V) was calculated. Ethanol was used as the displacing liquid. Briefly a sample of measured weight (W_i) was immersed in a graduated cylinder containing a known volume of ethanol and soaked for 24 h to allow ethanol to penetrate into the pores of the sponge. The final weight of the wet sponge was noted as W_f. Porosity can be calculated using the following equation.

$$\%\text{Porosity} = \left(\frac{(W_f - W_i)}{\rho_{ethanol} \times V}\right) \times 100$$

$\rho_{ethanol}$: density of ethanol

2.5. Swelling and water uptake studies

The swelling at different pH (4.0, 5.4, 6.8, 7.4 and 10.8) and water uptake ability of the composite sponges were studied in different buffer solutions and distilled water respectively. Dry weight of the sponges was noted as W_i. Sponges were immersed in buffer/water at 37 °C for different time points and then taken out and wet weight was taken as W_w, after removing the excess water with filter paper. Swelling ratio was determined using the formula

$$\text{Swelling ratio} = \frac{(W_w - W_i)}{W_i}$$

2.6. In vitro biodegradation studies

In vitro biodegradation of the sponges was studied in PBS (pH 7.4) with lysozyme (10^4 units/ml) (Fluka) at 37 °C. Preweighed (W_i) sponges were incubated at different time points. Samples were then taken out and washed with deionized water to remove the salts and freeze dried. Dry weight of the sponges was noted as W_d. Degradation percentage was calculated using the equation.

$$\%\text{Degradation} = \left[\frac{(W_i - W_d)}{W_i}\right] \times 100$$

2.7. Blood clotting studies

Blood drawn from human ulnar vein was mixed with anticoagulant acid citrate dextrose (ACD) at a ratio 9:1. The blood clotting efficiency of chitosan–HYA/nCS composite sponge was compared with chitosan–HYA sponges and commercially available Calcium Sodium Alginate Dressing, Kaltostat (ConvaTec). Samples of equal weight and size were used for the study. Blood without samples was used as blank. 200 μl of blood mixed with ACD was added to each sponge kept in a 24 well plate. To this 5 μl of 1% $CaCl_2$ was added to initiate blood clotting and incubated at 37 °C for 15 min. To hemolyze the red blood cells (RBC) that were not trapped in the

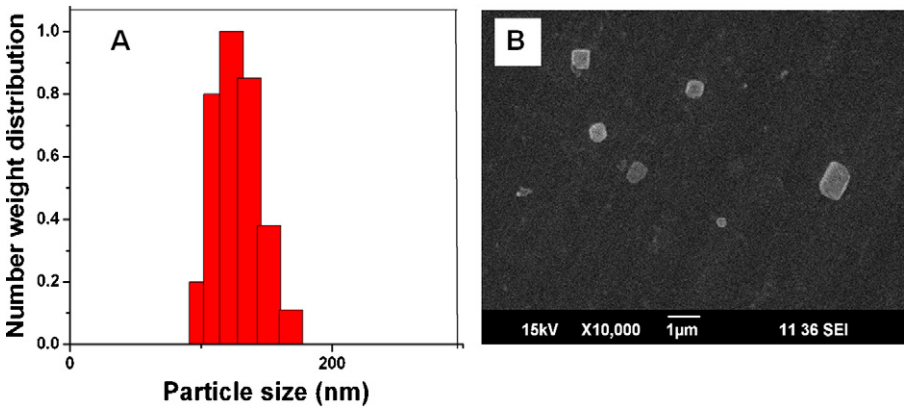

Fig. 1. (A) Particle size distribution and (B) SEM image of chondroitin sulfate nanoparticles.

clot 1 ml distilled water was added slowly along the sides of the plate without disturbing the clot (Ong, Wu, Moochhala, Tan, & Lu, 2008). 500 μl from this was centrifuged in an eppendorf for 2 min at 2000 rpm. Supernatant was collected and optical density at 540 nm was measured.

2.8. Platelet activation studies

For platelet activation studies blood mixed with anticoagulant was centrifuged at 2500 rpm for 10 min. Platelet rich plasma in supernatant was collected and added directly on to the sponge. Samples were fixed with glutaraldehyde, PBS washed, dehydrated using alcohol gradient and viewed under SEM.

2.9. Cell viability studies

Cell viability studies were done using alamar blue assay as per ISO specification 10993-5. EtO sterilized samples were used for the study. HDF cells (Promo cell) were seeded at a seeding density of 5×10^3 cells/sponge in a 96 well plate and incubated at different time points (24, 48, 72 and 96 h) at 37 °C and 5% CO_2. Alamar blue reagent diluted to 10% in fibroblast growth medium was added and after 6 h incubation absorbance was measured at 570 and 600 nm.

2.10. Cell attachment and proliferation studies

Cell attachment studies on the composite sponges were carried out using HDF cells for two different time points (12 and 48 h). EtO sterilized samples were used for the study. Cells were seeded on the sponges with a seeding density of 2×10^4 cells/sponge in a 24 well plate. After the incubation time the sponges were washed with PBS, fixed using 0.25% glutaraldehyde and dehydrated using alcohol gradient. The samples were then air dried, sputter-coated with gold and viewed under SEM.

For proliferation studies, after the culturing of HDF cells on the sponges for 24 and 48 h, the samples were stained with DAPI. Briefly, samples were washed with PBS, fixed with 4% paraformaldehyde, permeabilized using 0.5% Triton, blocked with 1% FBS and finally stained with DAPI (nuclear stain). The stained samples were imaged using fluorescent microscope (Olympus-BX-51).

3. Results and discussion

3.1. Preparation and characterization

nCS was prepared by the ionic cross-linking of chitosan and chondroitin sulfate. The prepared nCS was characterized using DLS and SEM (Fig. 1A and B). The particle size distribution of nCS showed a size range of 100–150 nm as shown in Fig. 1A. The average particle size as obtained from number average weight distribution was 128.3 nm. The particles showed a poly dispersity index of 0.28. The ternary composite sponge was prepared by mixing together chitosan hydrogel, HYA solution and nCS suspension. This composite gel was lyophilized, EDC cross-linked and relyophilized (Fig. 2).

SEM images showing the morphology of the prepared composite sponges are shown in Fig. 3A. Both chitosan–HYA and chitosan–HYA/nCS composite sponges showed an interconnected porous structure. Chitosan–HYA sponges showed more sheets like structures and irregular porous morphology where as the chitosan–HYA/nCS composite sponges showed a highly porous structure with uniform distribution of pores. This can be attributed to the vacant space generated after the removal of water by freeze drying from the nanoparticle suspension incorporated into the sponge. As HYA is water soluble the composite sponge will not be stable. In order to improve the stability, the sponges were cross-linked with EDC. It mediates amide bond formation between carboxyl group of HYA and amino group of chitosan. EDC is a zero length cross-linker and do not remain as part of the linkage. It forms water soluble urea derivatives which can be washed away and has low cytotoxicity as compared to other cross-linking agent such as glutaraldehyde (Park, Park, Kim, Song, & Suh, 2002).

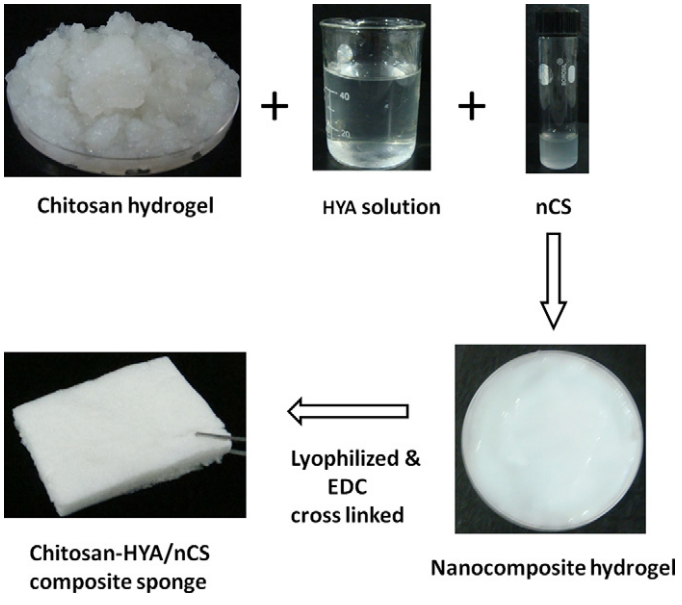

Fig. 2. Fabrication of chitosan–HYA/nCS composite sponge.

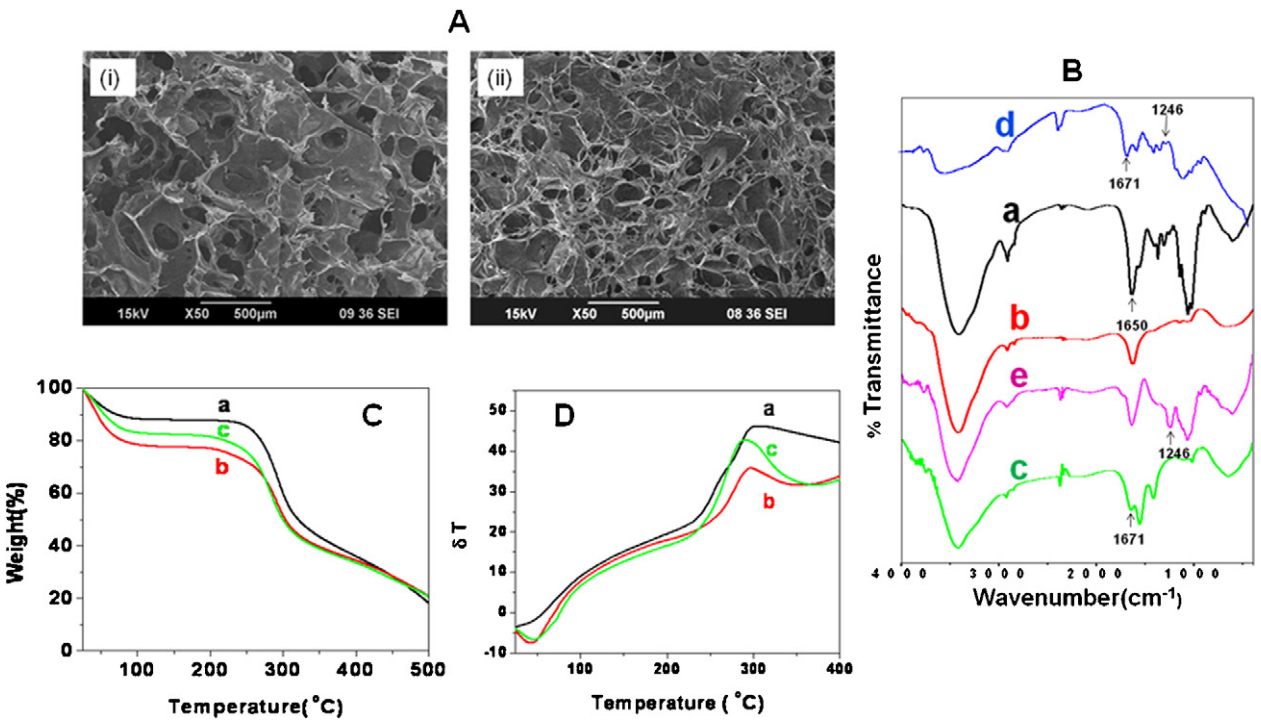

Fig. 3. (A) SEM image showing the porous morphology (i) chitosan–HYA sponge (ii) chitosan–HYA/nCS composite sponge. (B) FT-IR spectra of composite sponge (a) chitosan (b) HYA (c) chitosan–HYA (d) chitosan–HYA/nCS (e) chondroitin sulfate. (C) TG profile of composite sponge. (D) DTA profile (a) chitosan (b) chitosan–HYA (c) chitosan–HYA/nCS.

Fig. 3B shows the FTIR spectrum of composite sponge and the components. In chitosan–HYA and chitosan–HYA/nCS the amide bond band at 1650 cm^{-1} got shifted to 1671 cm^{-1}. This can be due to the cross-linking of carboxyl group of HYA and amino group of chitosan. Characteristic band of chondroitin sulfate at 1246 cm^{-1} corresponding to the S=O stretching can be seen in the chitosan–HYA/nCS composite which confirms the presence of nCS in the composite sponge (Park et al., 2002; Yeh et al., 2011).

Fig. 3C and D shows the thermogram of chitosan, chitosan–HYA and chitosan–HYA/nCS sponges. TG profile of composite sponges shows more degradation as compared to chitosan. Initial slope in the TG indicates water loss by evaporation and was found at around 50 °C. Decomposition at around 250 °C indicated the rupture of chains and degradation of polymer into monomer units. In DTA exothermic peak at around 300 °C indicates decomposition which correlates with the TG profile. An endothermic broad peak in the range of 30–60 °C was shown in chitosan whereas the composite sponges showed a peak at around 45 °C. This accounts for the loss of moisture by evaporation from the scaffold' which would explain the broad endothermic (Jayakumar, Nagahama, Furuike, & Tamura, 2008).

3.2. Porosity

Porosity studies of the composite sponges are shown in Fig. 4A. Chitosan–HYA/nCS sponges showed a porosity of 67% compared to the control which has a porosity of 50%. Since the chitosan–HYA/nCS sponge contains additional water content due to the incorporation of nanoparticle in the suspension form, lyophilization would yield a highly porous structure.

3.3. Swelling and water uptake studies

Fig. 4B and C shows the swelling and water uptake properties of chitosan–HYA and chitosan–HYA/nCS composite sponges in various pH buffers and water respectively. Nanocomposite sponges showed higher swelling and water uptake ability as compared to the control sponges. This can be due to the comparatively high porosity of the nanocomposite sponges. The swelling behavior of composite sponge was almost the same for all the pH. This shows the stability of the chitosan–HYA composite sponge despite of the pH of the solution. A possible reason for the stability of this composite can be the interaction of amine groups on chitosan with carboxyl groups on HYA which prevents the protonation of amino groups on chitosan (Li, Ramay, Hauch, Xiao, & Zhang, 2005).

3.4. In vitro biodegradation studies

In vitro biodegradation studies were done using lysozyme. Biodegradation profile of composite sponges is shown in Fig. 4D. nCS incorporated sponges showed a higher degradation profile as compared to the control sponges. The higher degradation ability of nanocomposite shows its potential to be used as an in situ biodegradable wound dressing.

3.5. Blood clotting and platelet activation studies

Whole blood clotting ability of the composite sponges is shown in Fig. 5A and B. RBCs that were not trapped in the clot were hemolyzed with water after contacting the samples with whole blood. Absorbance value of the resulting hemoglobin solution was noted at 540 nm. Higher absorbance value indicate slower clotting rate (Ong et al., 2008). As the absorbance value of chitosan–HYA/nCS sponges was lower than chitosan–HYA sponge and kaltostat the whole blood clotting ability of nCS incorporated sponges was good which holds an important property of an ideal wound dressing material. Platelet rich plasma after contacting with samples were fixed and viewed under SEM. More platelet activation was observed in chitosan–HYA/nCS sponges (Fig. 5C) which contributes to the blood clotting results.

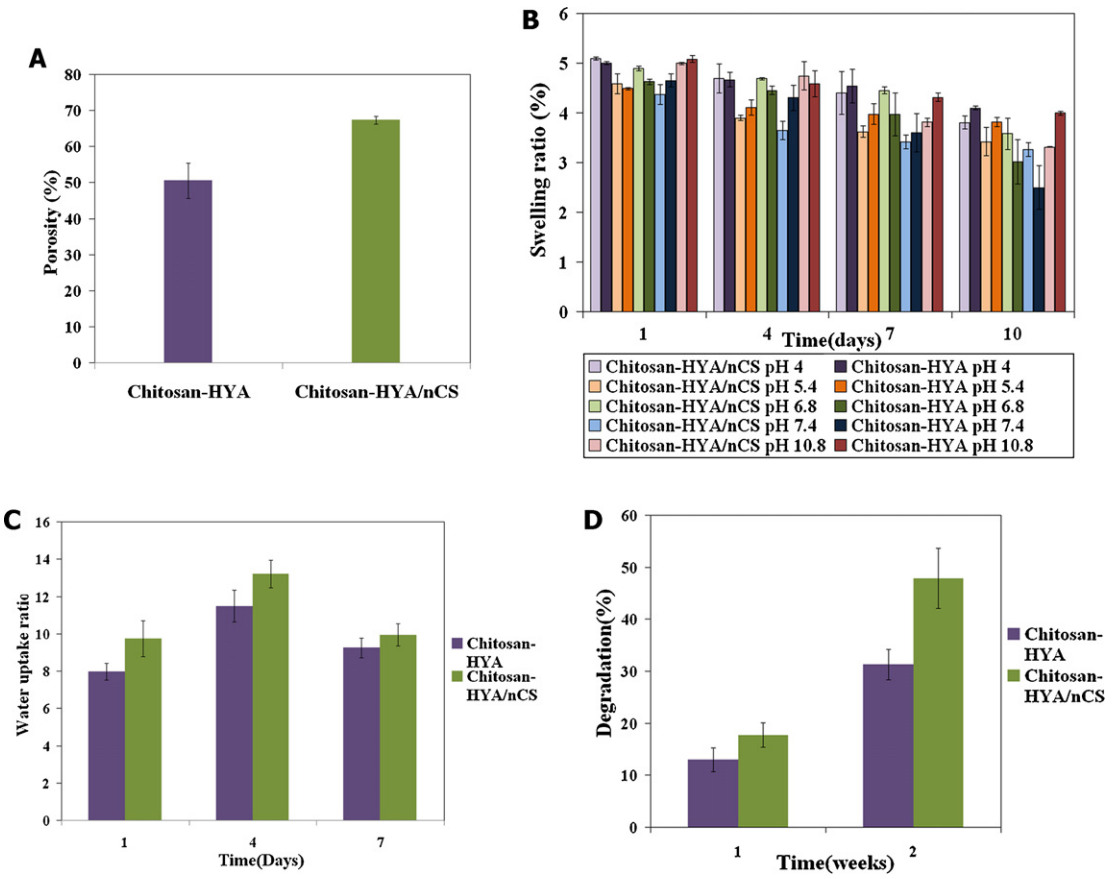

Fig. 4. (A) Porosity studies of composite sponge. (B) Swelling studies in various pH buffers. (C) Water uptake studies. (D) In vitro biodegradation studies of composite sponges in PBS containing lysozyme.

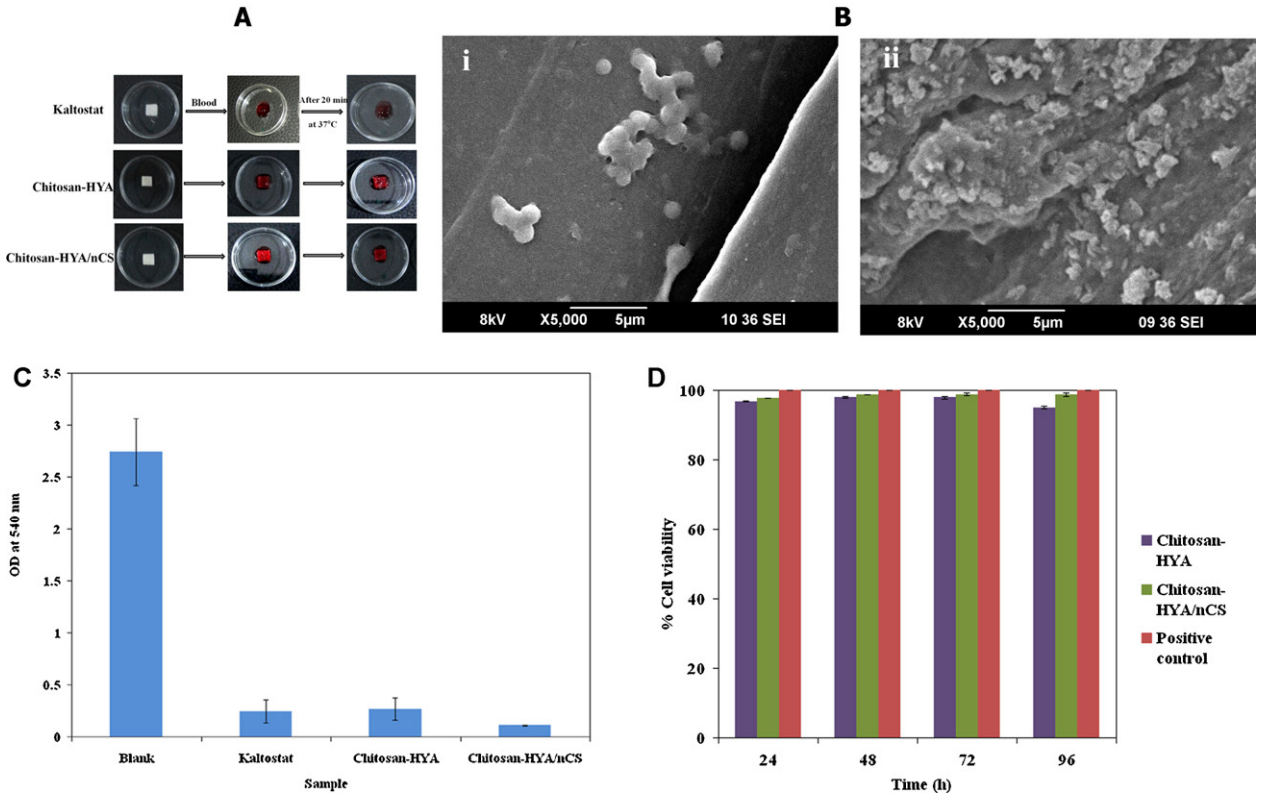

Fig. 5. (A) Optical image of whole blood clotting studies. (B) Blood clotting efficiency of composite sponges. (C) SEM images of platelet activation on (i) chitosan–HYA sponge and (ii) chitosan–HYA/nCS sponge. (D) Cell viability of HDF cells on samples at 24, 48, 72 and 96 h.

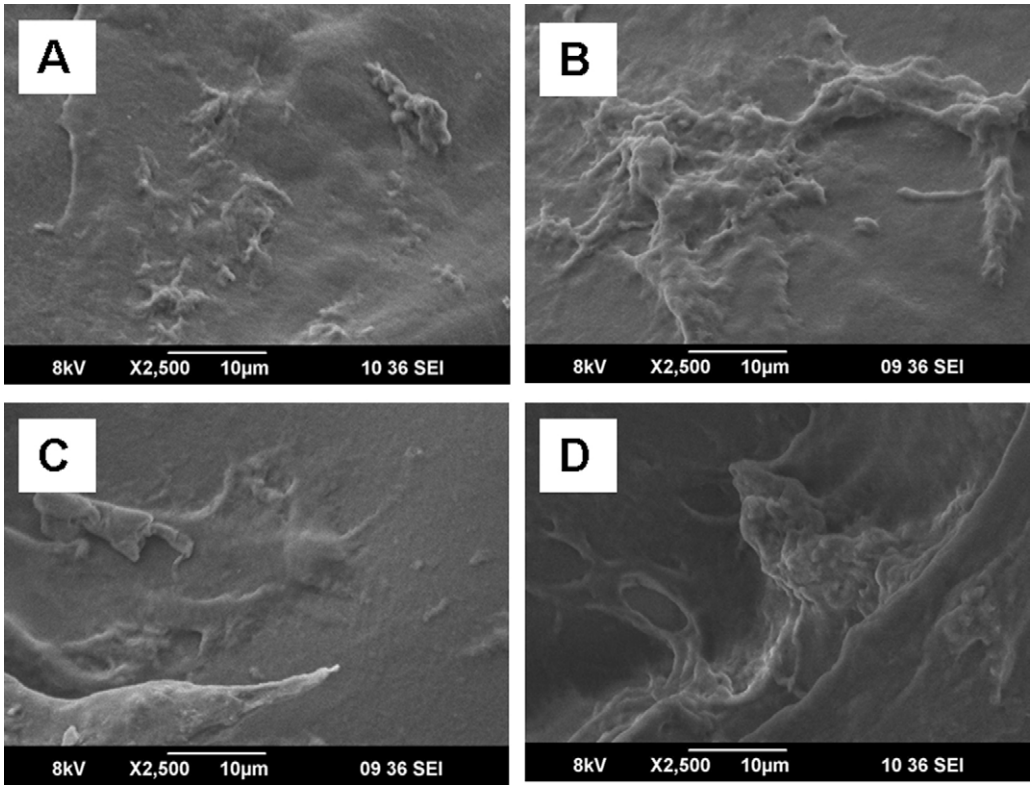

Fig. 6. SEM images of HDF cell attachment on sponges after 12 and 48 h of incubation on chitosan–HYA sponge (A and C) and chitosan–HYA/nCS nanocomposite sponge (B and D).

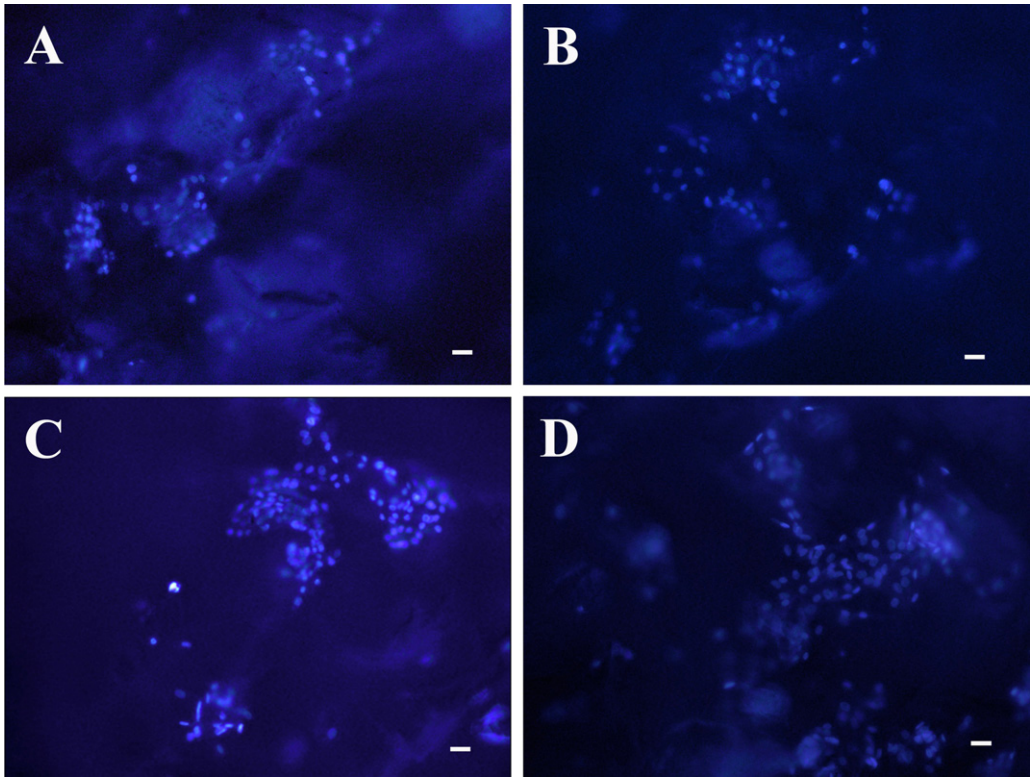

Fig. 7. Fluorescent microscopic images of HDF cells (nucleus stained blue with DAPI) after 24 and 48 h incubation on chitosan–HYA sponge (A and C) and chitosan–HYA/nCS nanocomposite sponge (B and D). Scale bar denotes 10 μm.

3.6. Cell viability studies

One of the most important parameter of a wound dressing is its nontoxic nature. Cell viability of HDF cells in presence of the composite sponges for 4 days was analyzed using alamar blue assay. The sponges showed more than 90% cell viability (Fig. 5D). It indicates that the prepared sponges were biocompatible.

3.7. Cell attachment and proliferation studies

Morphology and spreading patterns of cells on the sponges were obtained from SEM images after 12 and 48 h of seeding (Fig. 6A–D). Cells were well attached and showed excellent spreading on the nanocomposite sponges (Fig. 6B and D) compared to control sponges (Fig. 6A and C). This can be due to the higher surface to volume ratio of the nanoparticles which stimulates the interaction between the material and the cells. The elongated morphology observed in the cells seeded on the nanocomposite sponge after 48 h (Fig. 6D) is an indication of fibroblast migration which further facilitates faster wound healing. Fig. 7A–D shows the fluorescent microscopic images of nucleus stained cells on the sponges. DAPI staining clearly indicates a significant increase in cell number after 48 h in the nanocomposite sponge (Fig. 7D) compared to control sponge (Fig. 7C) highlighting the biocompatible nature of the same. The incorporation of nCS on the chitosan–HYA sponge could be the factor for the improved proliferation.

4. Conclusions

The developed chitosan–HYA/nCS composite sponge was characterized using SEM, FT-IR and TG-DTA. The nanocomposite sponge showed porosity in the range 60–70% which is adequate for a wound dressing. It also showed controlled swelling and biodegradation, enhanced blood clotting and platelet activation. Cytotoxicity studies using HDF cells proved the non toxic nature of composite sponges. The cell attachment and proliferation were qualitatively accessed using SEM and fluorescent microscopic image. An improved proliferation of the HDF cells were seen in the nanocomposite sponge and the SEM images explicit the elongated morphology of the cells. Thus the incorporation of nCS into chitosan–HYA sponge improved the overall efficacy of the sponge. In conclusion this chitosan–HYA/nCS composite sponge would be a potential candidate for wound dressing applications. As a future perspective nCS can be used as a delivery vehicle for growth factors to promote wound healing and it can be incorporated into chitosan–HYA sponge to further aid in wound healing.

Acknowledgements

One of the authors R. Jayakumar is grateful to Department of Biotechnology (DBT), India, for providing the fund (BT/PR13885/MED/32/145/2010 dated 03-01-2011). Dr. S.V. Nair and Dr. R. Jayakumar are also grateful to Nanomission, DST, India, which partially supported this work, under the Nanoscience and Nanotechnology Initiative program.

References

Anilkumar, T. V., Muhamed, J., Jose, A., Jyothi, A., Mohanan, P. V., & Krishnan, L. K. (2011). Advantages of hyaluronic acid as a component of fibrin sheet for care of acute wound. *Biologicals*, *39*, 81–88.

Boucard, N., Viton, C., Agay, D., Mari, E., Roger, T., Chancerelleb, Y., et al. (2007). The use of physical hydrogels of chitosan for skin regeneration following third-degree burns. *Biomaterials*, *28*, 3478–3488.

Collins, M. N., & Birkinshaw, C. (2011). Morphology of cross-linked hyaluronic acid porous hydrogels. *Journal of Applied Polymer Science*, *120*, 1040–1049.

Gilbert, M. E., Kirker, K. R., Gray, S. D., Ward, P. D., Szakacs, J. G., Prestwich, G. D., et al. (2004). Chondroitin sulfate hydrogel and wound healing in rabbit maxillary sinus mucosa. *Laryngoscope*, *114*, 1406–1409.

Jayakumar, R., Menon, D., Manzoor, K., Nair, S. V., & Tamura, H. (2010). Biomedical applications of chitin and chitosan based nanomaterials—A short review. *Carbohydrate Polymers*, *82*, 227–232.

Jayakumar, R., Nagahama, H., Furuike, T., & Tamura, H. (2008). Synthesis of phosphorylated chitosan by novel method and its characterization. *International Journal of Biological Macromolecules*, *42*, 335–339.

Jayakumar, R., Prabaharan, M., Sudheesh Kumar, P. T., Nair, S. V., & Tamura, H. (2011). Biomaterials based on chitin and chitosan in wound dressing applications. *Biotechnology Advances*, *29*, 322–337.

Kirker, K. R., Luo, Y., Nielson, J. H., Shelby, J., & Prestwich, G. D. (2002). Glycosaminoglycan hydrogel films as bio-interactive dressings for wound healing. *Biomaterials*, *23*, 3661–3671.

Kogan, G., Soltes, L., Stern, R., & Gemeiner, P. (2007). Hyaluronic acid: A natural biopolymer with a broad range of biomedical and industrial applications. *Biotechnology Letters*, *29*, 17–25.

Kondo, S., & Kuroyanagi, Y. (2012). Development of a wound dressing composed of hyaluronic acid and collagen sponge with epidermal growth factor. *Journal of Biomaterials Science Polymer Edition*, *23*, 629–643.

Li, Z., Ramay, H. R., Hauch, K. D., Xiao, D., & Zhang, M. (2005). Chitosan-alginate hybrid scaffolds for bone tissue engineering. *Biomaterials*, *26*, 3919–3928.

Madhumathi, K., Sudheesh Kumar, P. T., Abilash, S., Sreeja, V., Tamura, H., Manzoor, K., et al. (2010). Development of novel chitin/nanosilver composite scaffolds for wound dressing applications. *Journal of Materials Science: Materials in Medicine*, *21*, 807–813.

Mi, F. L., Shyu, S. S., Wu, Y. B., Lee, S. T., Shyong, J. Y., & Huang, R. N. (2001). Fabrication and characterization of a sponge-like asymmetric chitosan membrane as a wound dressing. *Biomaterials*, *22*, 165–173.

Muzzarelli, R. A. (2009). A chitins and chitosans for the repair of wounded skin, nerve, cartilage and bone. *Carbohydrate Polymers*, *76*, 167–182.

Muzzarelli, R. A. A., Greco, F., Busilacchi, A., Sollazzo, V., & Gigante, A. (2012). Chitosan, hyaluronan and chondroitin sulfate in tissue engineering for cartilage regeneration. A review. *Carbohydrate Polymers*, *89*, 723–739.

Nair, L. S., & Laurencin, C. T. (2007). Biodegradable polymers as biomaterials. *Progress in Polymer Science*, *32*, 762–798.

Ong, S. Y., Wu, J., Moochhala, S. M., Tan, M. H., & Lu, J. (2008). Development of a chitosan-based wound dressing with improved hemostatic and antimicrobial properties. *Biomaterials*, *29*, 4323–4332.

Park, S. N., Lee, H. J., Lee, K. H., & Suh, H. (2003). Biological characterization of EDC-crosslinked collagen-hyaluronic acid matrix in dermal tissue restoration. *Biomaterials*, *24*, 1631–1641.

Park, S. N., Park, J. C., Kim, H. O., Song, M. J., & Suh, H. (2002). Characterization of porous collagen/hyaluronic acid scaffold modified by 1-ethyl-3-(3-dimethylaminopropyl) carbodiimide cross-linking. *Biomaterials*, *23*, 1205–1212.

Peter, M., Binulal, N. S., Nair, S. V., Selvamurugan, N., Tamura, H., & Jayakumar, R. (2010). Novel biodegradable chitosan-gelatin/nano-bioactive glass ceramic composite scaffolds for alveolar bone tissue engineering. *Chemical Engineering Journal*, *158*, 353–361.

Shalumon, K. T., Anulekha, K. H., Sreeja, V. N., Nair, S. V., Chennazhi, K. P., & Jayakumar, R. (2011). Sodium alginate/poly(vinyl alcohol)/nano ZnO composite nanofibers for antibacterial wound dressings. *International Journal of Biological Macromolecules*, *49*, 247–254.

Wang, L., Khor, E., Wee, A., & Lim, L. Y. (2002). Chitosan-alginate PEC membrane as a wound dressing: Assessment of incisional wound healing. *Journal of Biomedical Materials Research*, *82*, 610–618.

Wang, W., Lin, S., Xiao, Y., Huang, Y., Tan, Y., Cai, L., et al. (2008). Acceleration of diabetic wound healing with chitosan-crosslinked collagen sponge containing recombinant human acidic fibroblast growth factor in healing-impaired STZ diabetic rats. *Life Sciences*, *82*, 190–204.

Yeh, M. K., Cheng, K. M., Hu, C. S., Huang, Y. C., & Young, J. J. (2011). Novel protein-loaded chondroitin sulfate-chitosan nanoparticles: Preparation and characterization. *Acta Biomaterialia*, *7*, 3804–3812.